

Intermolecular Double-Quantum-Coherence Imaging

S. Ahn,¹ R. R. Rizi,¹ T.-Q. Li,² L.-S. Bouchard,³ D. A. Roberts,¹ W. S. Warren,³ J. S. Leigh,¹ M. D. Schnall¹

¹Department of Radiology, MMRRCC, University of Pennsylvania Medical Center, Philadelphia, PA 19104

²Department of Psychology, ³Department of Chemistry, Princeton University, Princeton, NJ 08544

Introduction

Recently we have demonstrated a new type of MRI based on detection of intermolecular zero-quantum coherences (iZQCs) both *in vitro* and *in vivo*.^{1,2} These coherences correspond to simultaneously flipping two water spins in *opposite* directions on molecules separated by 10 μm – 10 mm. It is also possible to detect intermolecular double quantum coherences (iDQCs) corresponding to simultaneous flipping of two water spins in the *same* direction on distant molecules. The imaging of iDQCs was first demonstrated in coaxial tubes using a two-quantum CRAZED sequence,³ and recently in the cat brain.⁴ In this study, we show that phantom and human brain iDQC images are readily observable at 4T.

Methods

A spin-echo iDQC imaging sequence, consisting of two 90° pulses and a refocussing 180° pulse, is shown in Fig. 1. Two correlation gradient pulses are used to select iDQCs. Susceptibility variations of iDQCs (during τ_{DQ}) are refocused by a delay of $2\tau_{DQ}$ preceding the TE period. This setting will give the optimal condition to obtain the maximum signal.^{1,2} The

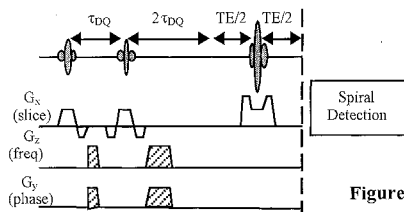


Figure 1

signal arises from pairs of nuclear spins, separated by approximately the "correlation distance" $d = \pi / (\gamma G_x T)$ which is half the repeat distance of the helix created by the correlation gradient.³ The resulting signal is sensitive to dynamic and structural variations on this distance scale. As discussed in the previous studies,⁵ a coherence transfer pathway for the iDQCs in the prototypical pulse sequence can be written briefly as

$$I_{\alpha} I_{\beta} \xrightarrow{-\pi/2} I_{\alpha}^{\dagger} I_{\beta}^{\dagger} \xrightarrow{-GT} I_{\alpha}^{\dagger} I_{\beta}^{\dagger} \exp(i2\gamma GT) \xrightarrow{-\pi/2} I_{\alpha} I_{\beta} \exp(i2\gamma GT) \xrightarrow{-2GT} \frac{D_{\alpha}^{\dagger} I_{\beta}}{I_{\alpha}} \quad (1)$$

With uniform magnetization, and ignoring both relaxation and inhomogeneous broadening, the exact signal at the echo time TE obtained from either the quantum or classical treatment is

$$M^* = iM_0 2(\tau_d / \Delta_s (TE + 2\tau_{DQ})) J_2(-\Delta_s (TE + 2\tau_{DQ}) / \tau_d); \quad (2)$$

$$\Delta_s = \{3(\hat{s} \cdot \hat{z}) - 1\} / 2, \quad \tau_d = (\mu_0 M_0)^{-1}$$

where the dipolar demagnetizing time is 240 ms for pure water at room temperature in a 4T magnet. In realistic imaging applications, the iDQC signal is weaker than a conventional image due to relaxation and inhomogeneity. Therefore, the real utility of the iDQC images comes from different contrast.

Results and Discussion

In Figure 2 iDQC images of a silicone oil phantom are shown as a function of echo time which show an increase in signal intensity up to an echo time of 150–200 ms followed by decreasing signal. In general, multiple-quantum dipolar field effects are proportional to $3\cos^2\theta - 1$ where θ is the angle

between the correlation gradient direction and the dipolar field. Figure 3 illustrates the gradient direction effects (z vs y ; TE=150 ms), which can verify that the signal is not contaminated by conventional signal or stimulated echoes.

Figure 4 shows human brain images (TE = 20ms, 50 ms), which also show an increase in signal intensity for the longer TE. In general, as discussed elsewhere,^{1,2} iDQC images may give relatively poorer contrast than iZQC images due to dephasing effects of DQCs during the evolution period (twice the conventional single quantum coherences). However, the iDQC-imaging will be more sensitive to motion and flow. The clinical utility of iDQC imaging remains to be validated. We are currently evaluating this pulse sequence for fMRI studies.

Figure 2. iDQC images of Si phantom, taken for a fixed τ_{DQ} (10ms) and different TE's (15, 40, 70, 100, 150, 200, 300 and 400 ms from top left).

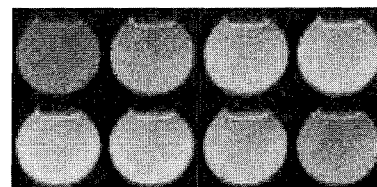


Figure 3 Z Y

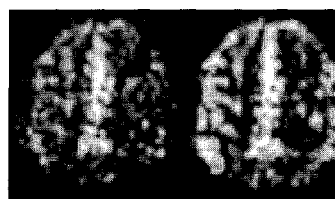
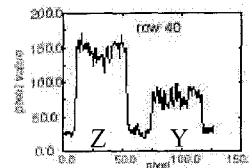


Figure 4. iDQC images of human brain with different TE's, 20 ms (left) and 50 ms (right) : matrix size 64x64, slice thickness 8 mm, number of signal accumulations 64, TR 5 s and τ_{DQ} 10ms.

Acknowledgement

Part of this research is being supported by a NIH supported Resource Center (RR02305, Penn) and GM35253 (Princeton).

References

1. W. S. Warren *et al.*, *Science* **281**, 247 (1998).
2. R. R. Rizi *et al.*, *Magn. Reson. Med.* (submitted).
3. W. Richter *et al.*, *Science* **267**, 654 (1995).
4. S. Mori *et al.*, *Magn. Reson. Med.* **37**, 336-340 (1997).
5. S. Lee *et al.*, *J. Chem. Phys.* **105**, 874 (1996).